Performance Comparison for Signal Amplitude Analysis Algorithms in nano biosensor application

Teh Yi Jun[1], Asral Bahari Jambek[2] and Uda Hashim[3]
[1,2]*School of Microelectronic Engineering, Universiti Malaysia Perlis, Perlis, Malaysia*
[3]*Insituite of Nano Electronic Engineering, Universiti Malaysia Perlis, Perlis, Malaysia*
Email: [1]kelvinteh90@gmail.com, [2]asral@unimap.edu.my, [3]uda@unimap.edu.my

***Abstract*—This paper analyses the performance of various signal amplitude analysis algorithms. Five algorithms are reviewed: automatic threshold peak detection (ATPD), automatic chromatographic peak detection (ACPD), adaptive threshold method (ATM), peak of Shannon energy envelope (PSEE), and automatic multiscale peak detection (AMPD). The selected algorithms are potential method for nano biosensor application. These algorithms are investigated for periodic and non-periodic signal. Based on the experiment results, the ATPD gives the lowest detection error(33%). In terms of computational speed, the ATM method is fastest, with a speed at least two times that of any of the other algorithms.**

***Index Terms*—Nano-bio Sensor, Bio sensor signal anlysis.**

I. Introduction

Over the past decade, the importance of nano-technologies has grown rapidly[1]. Such technologies provide huge advantages in nanoscale biosensors[2], allowing these sensors to improve their sensitivity and selectivity. These nano-biosensors can provide various signal responses, such as changes in amplitude, frequency, phase, and time interval. Different signal responses require different algorithms. Efficient signal analysis algorithms are therefore required to support the growth of nanoscale biosensors.

In conventional methods, signal analysis is performed by a human using an off-chip device. This approach contains the potential for human error; moreover, it is expensive, time-consuming and not suitable for portable lab-on-chip application[3]. With the growth of system-on-chip (SoC) technology[4], [5], it is possible to develop an automatic on-chip analyser for nano-biosensors.

This paper discusses various algorithms that analyse signal amplitude generated by sensors. Five algorithms are selected and their performance characteristics are evaluated in terms of sensitivity, positive prediction, error detection, and computational speed. The rest of the paper is organized as follows. Section II reviews existing amplitude signal analysis algorithms. Section III elaborates our experimental procedure to measure the performance of these algorithms. The results of our experiment are presented in Section IV. Section V provides conclusions.

II. Literature Review

In this section, five existing methods of amplitude signal analysis will be discussed. The authors in [6] proposed R-peak detection of ECG signals based on peak of Shannon energy envelope (PSEE). Fig. 1 shows the peak detection for real-time ECG signal. Fig. 2 presents a block diagram of the peak of Shannon energy envelope (PSEE) system. This method is used to monitor and analyse real-time electrocardiograms (ECG). This method consists of three stages: data preparation, SEE extraction, and peak finding. In the data preparation stage, the raw ECG signal is processed using a band-pass filter, differencing, and amplitude transforming. In the SEE extraction stage, the signal from the preparation stage will pass into Shannon transformation and low-pass filtering. The objective at this stage is to envelope the signal using SEE. The output will then pass into the peak finding stage, where the analysis involves peak detection (PD), false-R detection (FRD), and false-noise detection (FND). The overall accuracy of this system can reach above 99.83%.

The authors in [7] proposed an adaptive threshold method (ATM) for peak detection of photoplethysmography (PPG)-based temporal analyses. This method is used for physiological and cardiovascular diagnosis, including of changes in blood volume. It consists of two parts: adaptive threshold detection, and peak correction. Fig. 3 illustrates the method. In the adaptive threshold detection part, the virtual threshold will be increased or decreased with a fixed slope parameter to detect the trough and peak. This step is repeated with various slopes until every peak is found. In Fig. 3(a), the solid line is the bandpass-filtered PPG waveform and the dashed line is the detection threshold. Fig. 3(b) illustrates if the detected peak is found in the refractory period is ignored, and the threshold level is not affected by ignored peaks. The results show that this PPG waveform can achieve 98.22% accuracy.

The authors in [8] proposed an automatic chromatographic peak detection (ACPD) method. This is used to analyse chromatographic fingerprints of complex samples, including botanical extracts and urine samples. Fig. 4 illustrates the framework of automatic chromatographic peak detection. This method consists of five stages: preliminary chromatographic peak detection, automatic instrumental noise-level estimation, pseudo-peak elimination, chromatographic peak clustering, and peak baseline estimation and small-peak elimination. First, the signal is processed in the preliminary chromatographic peak detection stage. In this stage, every peak start position and end position is found. Then, the signal is processed in the automatic instrumental noise-level estimation stage. In this stage, the

Published Manuscript Link: http//10.1109/IECBES.2016.7843454

978-1-4673-7791-1/16/$31.00 ©2016 IEEE

instrumental noise level and threshold value for the first-order derivative are calculated. Example results are shown in Fig. 4 (C). Then, false peaks are eliminated in the pseudo-peak elimination stage, based on the threshold value. Then, the chromatographic peak clustering and peak baseline estimation stage calculates the average signal-to-noise ratio. Finally, peaks with ASNR smaller than the instrumental noise level are eliminated in the small-peak elimination stage.

The authors in [4] and [5] proposed the auto-threshold peak detection (ATPD) method for portable multi-model nano-biosensor systems and physiological signal detection. Fig. 5illustrates peak detection for the final output of a noisy signal using the auto-threshold algorithm. This method consists of two stages: cluster mean calculation, and peak detection. In the cluster mean calculation stage, the sample is assigned to the nearest cluster mean; the new cluster mean is determined after all samples have been assigned. This step is repeated until the cluster mean is less than the termination condition. In the peak detection stage, the larger cluster mean will be used as the threshold value. A peak is defined when the local maxima are between a leading edge and falling edge when the edge is larger than the threshold value.

The authors in [11] proposed an automatic multiscale-based peak detection (AMPD) method for automatic peak detection in noisy periodic and quasi-periodic signals. This method is applicable to many real-world signals, including blood volume in functional near-infrared spectroscopy (fNIRS) signal, and maximum concentration of expired CO_2 and QRS peaks in ECG signal. Fig. 6 illustrates the calculation steps of the AMPD algorithm. This method consists of four steps: local maxima scalogram (LMS) calculation, row-wise summation of the LMS, LMS rescaling, and peak detection. Fig. 7 shows an example of application of the AMPD algorithm to a simulated signal. The first step is the LMS calculation. In this step, the local maxima are determined using a moving-window approach. Then, a matrix is formed based on the LMS of the signal. Fig. 7(a) illustrates the LMS. After that, the row-wise summation of the LMS step is performed. In this step, the algorithm performs a row-wise summation of the LMS matrix. Fig. 7(c) illustrates the row-wise summation of each row. Next, the LMS rescaling step is used to reshape the LMS matrix according to the row of lowest row-wise summation. Fig. 7(b) illustrates the rescaled LMS. In the last step, the peaks are determined by calculating the column-wise standard deviation of the matrix after reshaping. Fig. 7(d) shows the calculated row-wise standard deviation of the rescaled LMS. Figs. 7(e) and (f) show the detected peaks.

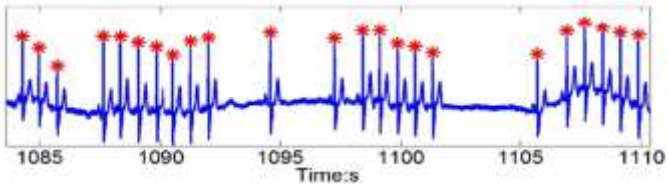

Fig. 1. Peak detection for ECG signal [6].

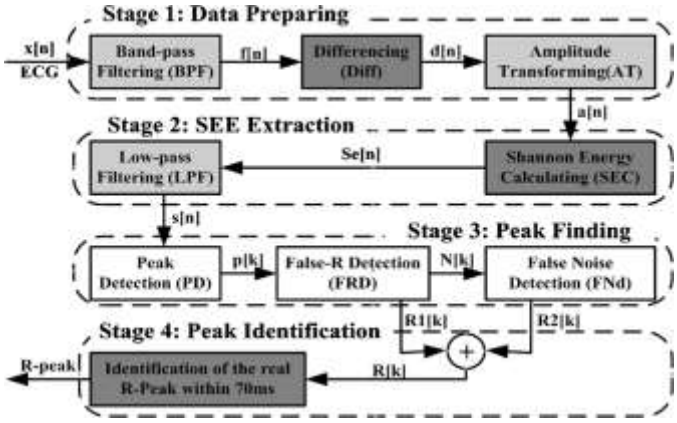

Fig. 2. Block diagram of the PSEE. The deep grey, shallow grey, and white backgrounds indicate original, improved, and newly introduced parts, respectively [6].

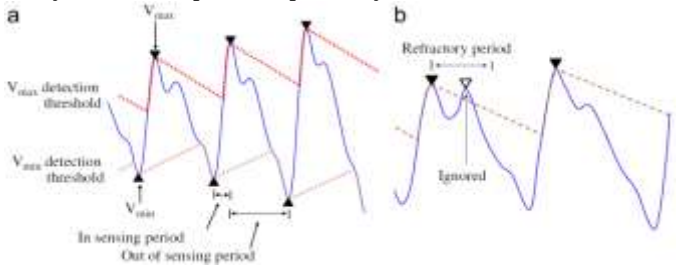

Fig. 3. Adaptive threshold method[7].

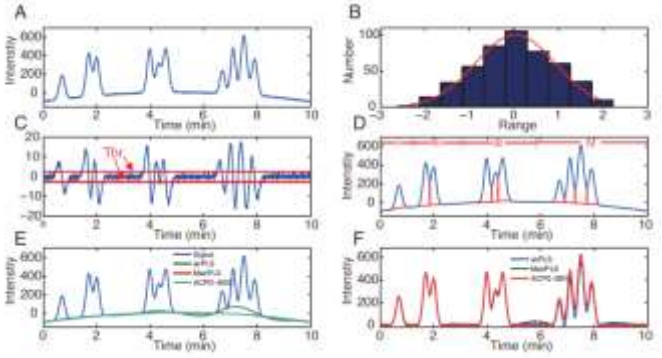

Fig. 4. ACPD signal processing stage [8].

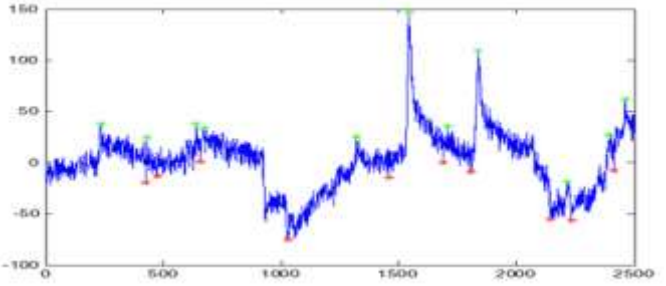

Fig. 5. Peak detection results of auto-threshold algorithm[9].

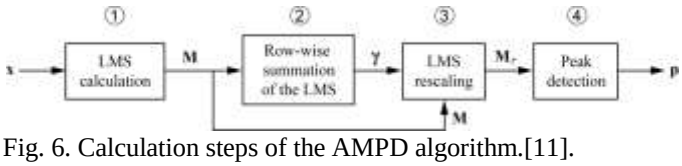

Fig. 6. Calculation steps of the AMPD algorithm.[11].

Published Manuscript Link: http//10.1109/IECBES.2016.7843454

978-1-4673-7791-1/16/$31.00 ©2016 IEEE

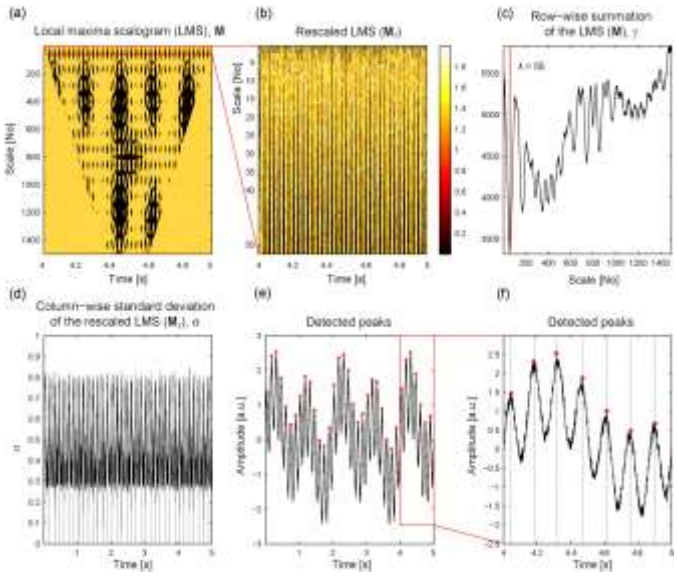

Fig. 7. Example of application of the AMPD algorithm to a simulated signal [11].

III. Methodology

In Section II, five algorithms have been discussed. Next, the accuracy of these algorithms is simulated in a Matlab environment (MathWorks, USA) using a computer with Win8 (64-bit) Intel®Core™i7 CPU (2.4 GHz, 8 G RAM). The simulation is carried out for periodic and non-periodic signal. For the periodic signal, ECG signal from the PhysioNet database is used; the non-periodic signal is a segment of ECG signal where only a circle of it without repetition QRS peak. The purpose of this is to identity the ability of algorithms to perform peak detection for only one period cycle signal. The signal is classified under best, typical, and worst case. This classification is based on the standard deviation of the peak value. High standard deviation of peak value will be classified as worst case, moderate standard deviation of peak value will be classified as typical, and low standard deviation of peak value will classified as best case.

Fig. 8, Fig. 9, and Fig. 10 show the actual peak in the periodic signal for the best, worst, and typical cases, respectively. Fig. 11, Fig. 12, and Fig. 13 show the actual peak in the non-periodic signal for the best case, worst case, and typical case, respectively. The actual peak is defined based on the theory of QRS peaks of ECG signal. Table 1 summarizes the total peak number for each signal. For periodic signal, the best case has five peaks, the worst case 22 peaks, and the typical case six peaks. For non-periodic signal, the best case has one peak, the worst case four peaks, and the typical case one peak.

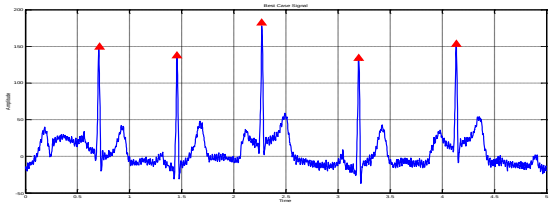

Fig. 8. Peaks for best-case periodic signal.

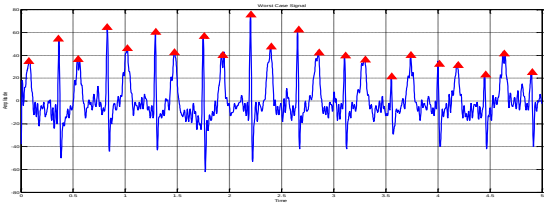

Fig. 9. Peaks for worst-case periodic signal.

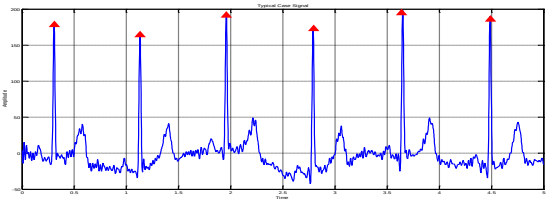

Fig. 10. Peaks for typical-case periodic signal.

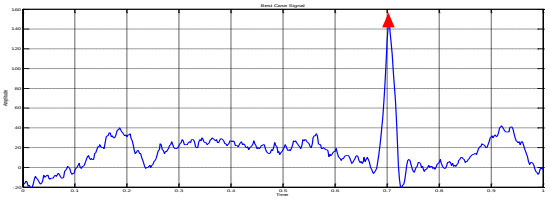

Fig. 11. Peaks for best-case non-periodic signal.

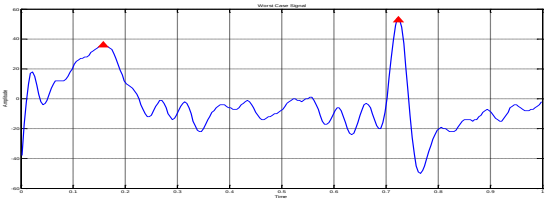

Fig. 12. Peaks for worst-case non-periodic signal.

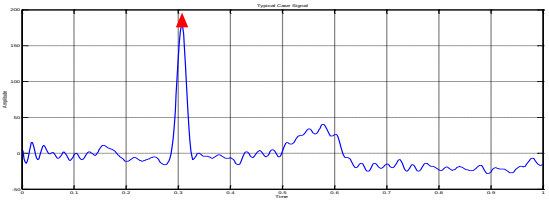

Fig. 13. Peaks for typical-case non-periodic signal.

Table 1. Total signal peaks.

Signal		Total Peak Number
Periodic	Best	5
	worst	22
	typical	6
Non-Periodic Signal	Best	1
	worst	4
	typical	1

IV. Result and Discussions

This section discusses the experimental results to compare the performance of the ATPD, PSEE, ATM, ACPD, and AMPD algorithms. First, we will present the sensitivity (Se%) and positive detection (+P%), followed by the detection error

Published Manuscript Link: http//10.1109/IECBES.2016.7843454

978-1-4673-7791-1/16/$31.00 ©2016 IEEE

(DER%) for each algorithm. Next, we will compare the computational speeds required to complete the task for each method.

Figs. 14 to 18 show the results for typical-case periodic signal, while Figs. 19 to 23 show the results for typical-case non-periodic signal. Note that due to limited space, the results for the best and worst cases are not shown here. Each peak detected by the algorithms is labelled by a triangle shape in the figures. From the figures, it can be seen that all algorithms are able to detect peaks with different levels of performance.

To evaluate the performance of the peak detection algorithms, we use three benchmark parameters: positive prediction (+P), sensitivity (SE), and detection error (DER). To calculate +P, SE, and DER we include the false negative (FN), which represents failure to detect a true peak (peak not detected as a peak), the false positive (FP), which means false peak detection (non-peak detected as a peak). Then, +P, SE, and DER can be calculated as shown in Eqs. (1), (2), and (3), respectively, as suggested by[12]–[15].

$$+P = \frac{TP}{TP+FP} \quad (1)$$

$$SE = \frac{TP}{TP+FN} \quad (2)$$

$$DER = \frac{FP+FN}{TPN} \quad (3)$$

TP is the number of true positive detections (peak detected as a peak), while TPN is the total number of peaks in a signal. +P reports the percentage of peak detections that are true peaks. SE reports the percentage of true peaks that are correctly detected by the algorithm. DER reports the percentage of peak detection error.

Table 2 summarizes the +P, SE, and DER values for each algorithm based on the experimental results. For only periodic signal, ATPD gave the lowest DER, 27%; however, for only non-periodic signal, ATM achieved the lowest DER, 25%. This means ATPD works better for periodic signal while ATM works better for non-periodic signal.

In terms of the overall results, ACPD and PSEE have the highest +P, both achieving 100%. This means all the peaks detected by ACPD and PSEE are true peaks. However, FN still occurs with ACPD and PSEE. For SE, ACPD achieved 54% and PSEE achieved 59%. ATPD has the highest SE, 100%. This means no true peaks went undetected. However, FP still occurs. ATPD achieved 74% +P and achieved the lowest DER, 35%. This means ATPD has the highest accuracy of peak detection.

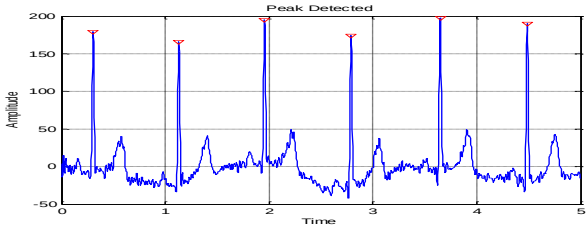

Fig. 14. Peak detection for typical-case periodic signal using ACPD.

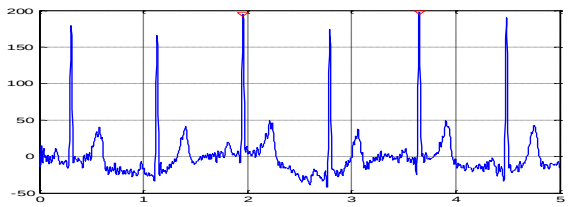

Fig. 15. Peak detection for typical-case periodic signal using AMPD.

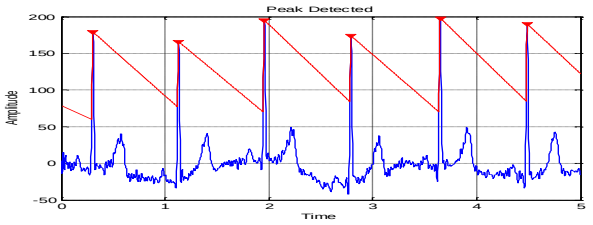

Fig. 16. Peak detection for typical-case periodic signal using ATM.

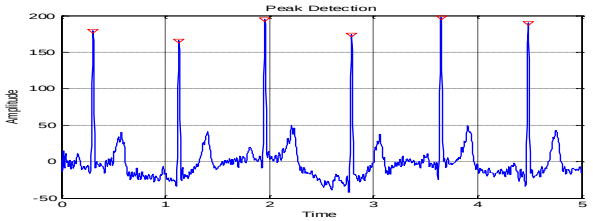

Fig. 17. Peak detection for typical-case periodic signal using ATPD.

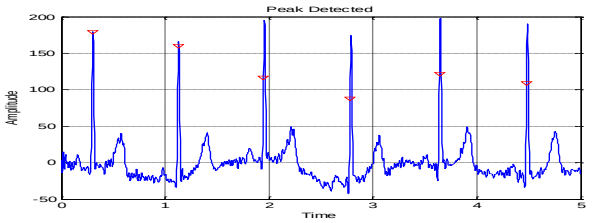

Fig. 18. Peak detection for typical-case periodic signal using PSEE.

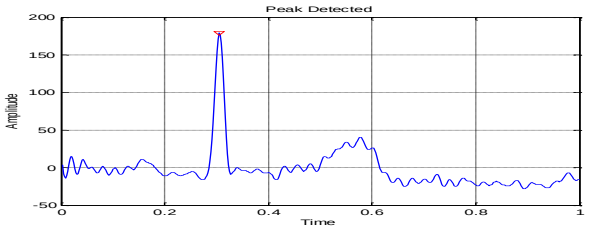

Fig. 19. Peak detection for typical-case non-periodic signal using ACPD.

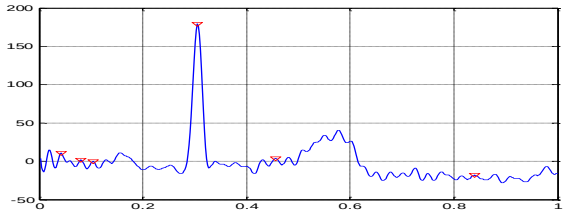

Fig. 20. Peak detection for typical-case non-periodic signal using AMPD.

Published Manuscript Link: http//10.1109/IECBES.2016.7843454

978-1-4673-7791-1/16/$31.00 ©2016 IEEE

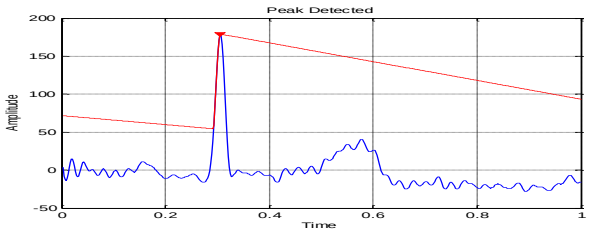

Fig. 21. Peak detection for typical-case non-periodic signal using ATM.

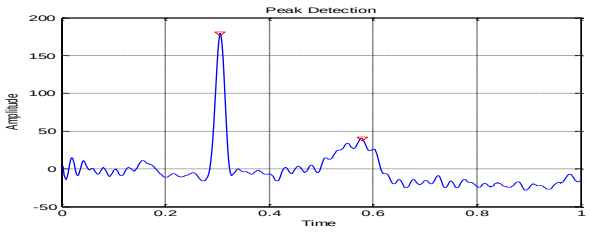

Fig. 22. Peak detection for typical-case non-periodic signal using ATPD.

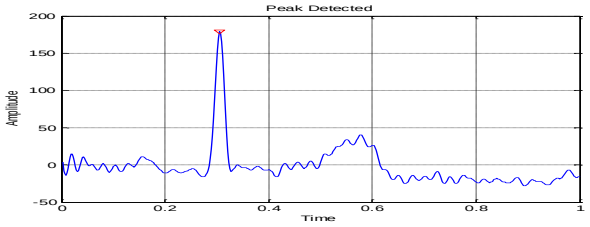

Fig. 23. Peak detection for typical-case non-periodic signal using PSEE.

Table 2. Comparison of peak detection performance with raw signal.

Method	Signal Type	Signal Case	Total Peak Number	Actual Peak Detected	Actual Peak Missing	False Peak Detected	SE%	+P%	DER%
ACPD	Periodic Signal	Best	5	5	0	0	100%	100%	0%
		Worst	22	6	16	0	27%	100%	73%
		Typical	6	6	0	0	100%	100%	0%
		Total	33	17	16	0	52%	100%	48%
	Non-Periodic Signal	Best	1	1	0	0	100%	100%	0%
		Worst	2	1	1	0	50%	100%	50%
		Typical	1	1	0	0	100%	100%	0%
		Total	4	3	1	0	75%	100%	25%
	Total		37	20	17	0	54%	100%	46%
AMPD	Periodic Signal	Best	5	3	2	144	60%	2%	2920%
		Worst	22	9	13	0	41%	100%	59%
		Typical	6	2	4	0	33%	100%	67%
		Total	33	14	19	144	42%	9%	494%
	Non-Periodic Signal	Best	1	1	0	25	100%	4%	2500%
		Worst	2	2	0	1	100%	67%	50%
		Typical	1	1	0	5	100%	17%	500%
		Total	4	4	0	31	100%	11%	775%
	Total		37	18	19	175	49%	9%	524%
ATM	Periodic Signal	Best	5	5	0	0	100%	100%	0%
		Worst	22	12	10	2	55%	86%	55%
		Typical	6	6	0	0	100%	100%	0%
		Total	33	23	10	2	70%	92%	36%
	Non-Periodic Signal	Best	1	1	0	1	100%	50%	100%
		Worst	2	2	0	0	100%	100%	0%
		Typical	1	1	0	0	100%	100%	0%
		Total	4	4	0	1	100%	80%	25%
	Total		37	27	10	3	73%	90%	35%
ATPD	Periodic Signal	Best	5	5	0	8	100%	38%	160%
		Worst	22	22	0	1	100%	96%	5%
		Typical	6	6	0	0	100%	100%	0%
		Total	33	33	0	9	100%	79%	27%
	Non-Periodic Signal	Best	1	1	0	3	100%	25%	300%
		Worst	2	2	0	0	100%	100%	0%
		Typical	1	1	0	1	100%	50%	100%
		Total	4	4	0	4	100%	50%	100%
	Total		37	37	0	13	100%	74%	35%
PSEE	Periodic Signal	Best	5	5	0	0	100%	100%	0%
		Worst	22	8	14	0	36%	100%	64%
		Typical	6	6	0	0	100%	100%	0%
		Total	33	19	14	0	58%	100%	42%
	Non-Periodic Signal	Best	1	1	0	0	100%	100%	0%
		Worst	2	1	1	0	50%	100%	50%
		Typical	1	1	0	0	100%	100%	0%
		Total	4	3	1	0	75%	100%	25%
	Total		37	22	15	0	59%	100%	41%

Table 3. Comparison of computational-speed normalization with ATM.

		ATM	ATPD	ACPD	PSEE	AMPD
Periodic	Best	1.00	1.81	2.67	4.95	327.98
	Worst	1.00	2.39	2.37	4.65	306.78
	Typical	1.00	3.31	2.38	4.52	297.06
	Average of Periodic	**1.00**	**2.53**	**2.47**	**4.70**	**310.03**
Non-Periodic Signal	Best	1.00	1.44	1.24	3.98	15.42
	Worst	1.00	1.47	1.47	3.69	13.56
	Typical	1.00	1.37	1.63	3.86	13.97
	Average of Non-Periodic	**1.00**	**1.43**	**1.43**	**3.85**	**14.41**
	Average	**1.00**	**2.05**	**2.00**	**4.33**	**175.19**

Published Manuscript Link: http//10.1109/IECBES.2016.7843454

978-1-4673-7791-1/16/$31.00 ©2016 IEEE

The comparison of normalized computational speeds mentioned in Section II is shown in Table 3. This speed is calculated based on the total time taken by the algorithm to complete the task in the Matlab simulation. For the periodic signal, the results show that ATM provides the fastest speed, followed by ACPD, ATPD, PSEE, and AMPD. ATM is about 2.5 times faster than ATPD and ACPD, about 4.7 times faster than PSEE, and about 310 times faster than AMPD. A similar pattern can also be observed for non-periodic-signal computation speed. The results show that ATM achieved the shortest processing time for this type of signal.

The reason ATM is able to achieve the lowest computational time is that the algorithm has low complexity, only calculating the slope of the signal to determine the signal peaks. The other methods require more effort to detect the peaks. For example, AMPD needs to pre-construct the LMS matrix, and therefore takes more time to detect the peaks.

Algorithms with high complexity require more time to complete detection. This will translate into higher power consumption when implemented on a chip. For lab-on-chip implementation, lower-computational-load algorithms are preferred to reduce the energy consumption. Based on the experimental results, ATPD gives the best trade-off of these five algorithms between accuracy and speed. The algorithm is able to provide the highest accuracy at moderate speed and with moderate power consumption.

V. Conclusions

In this paper, the performance of five peak detection algorithms has been analysed and compared: automatic threshold peak detection (ATPD), automatic chromatographic peak detection (ACPD), adaptive threshold method (ATM), peak of Shannon energy envelope (PSEE), and automatic multiscale peak detection (AMPD). These algorithms have been tested using various periodic and non-periodic signals to measure their performance and computational speed. Based on the experimental results, ATPD is able to provide the highest detection accuracy, with moderate computational load.

VI. 6. Acknowledgements

This research was supported by the Fundamental Research Grant Scheme, Ministry of Higher Education, Malaysia (FRGS Phase 1, 2014).

References

[1] N. Sozer and J. L. Kokini, “Nanotechnology and its Applications in the Food Nanotechnology and its applications in the food sector,” *Trends Biotechnol.*, vol. 27, no. 2, pp. 82–89, 2009.

[2] J.L. Arlett, E.B. Myers, and M.L. Roukes*, “Comparative Advantages of Mechanical Biosensors,” *Nat. Nanotechnol.*, vol. 6, no. 4, pp. 203–215, 2011.

[3] P Abgrall and A-M Gue, “Lab-on-chip technologies : making a microfluidic network and coupling it into a complete microsystem — a review,” *J. Micromechanics Microengineering*, vol. 17, no. 5, pp. R15–R49, 2007.

[4] D. Lyonnard, S. Yoo, A. Baghdadi, and Ahmed A. Jerraya, “Automatic Generation of Application-Specific Architectures for Heterogeneous Multiprocessor System-on-Chip,” in *Proceedings of the 38th annual Design Automation Conference*, 2001, pp. 518–523.

[5] T. A. C. M. Claasen, “An Industry Perspective on Current and Future State of the Art in System-on-Chip (SoC) Technology,” in *Proceedings of the IEEE*, 2006, vol. 94, no. 6, pp. 1121 – 1137.

[6] H. Zhu and J. Dong, “An R-peak detection method based on peaks of Shannon energy envelope,” *Biomed. Signal Process. Control*, vol. 8, no. 5, pp. 466–474, Sep. 2013.

[7] H. S. Shin, C. Lee, and M. Lee, “Adaptive threshold method for the peak detection of photoplethysmographic waveform.,” *Comput. Biol. Med.*, vol. 39, no. 12, pp. 1145–52, Dec. 2009.

[8] Y.-J. Yu, Q.-L. Xia, S. Wang, B. Wang, F.-W. Xie, X.-B. Zhang, Y.-M. Ma, and H.-L. Wu, “Chemometric strategy for automatic chromatographic peak detection and background drift correction in chromatographic data.,” *J. Chromatogr. A*, vol. 1359, pp. 262–70, Sep. 2014.

[9] J. Park, J. Song, H. Kim, and D. Ryu, “Peak Detection for Portable Multi-modal Nano-bio Sensor System,” *Int. J. Bio-Science Bio-Technology*, vol. 5, no. 3, pp. 135–142, 2013.

[10] a. L. Jacobson, “Auto-threshold peak detection in physiological signals,” *2001 Conf. Proc. 23rd Annu. Int. Conf. IEEE Eng. Med. Biol. Soc.*, vol. 3, pp. 2194–2195, 2001.

[11] F. Scholkmann, J. Boss, and M. Wolf, “An Efficient Algorithm for Automatic Peak Detection in Noisy Periodic and Quasi-Periodic Signals,” *Algorithms*, vol. 5, no. 4, pp. 588–603, Nov. 2012.

[12] M. Merah, T. A. Abdelmalik, B. H. Larbi, E. M. Naouar, and B. D.- Oran, “R-peaks detection based on stationary wavelet,” *Comput. Methods Programs Biomed.*, vol. 121, no. 3, pp. 149–160, 2015.

[13] J. P. Martínez, R. Almeida, S. Olmos, A. P. Rocha, and P. Laguna, “A Wavelet-Based ECG Delineator : Evaluation on Standard Databases,” *IEEE Trans. Biomed. Eng.*, vol. 51, no. 4, pp. 570–581, 2004.

[14] V. X. Afonso and W. J. Tompkins, “ECG Beat Detection Using Filter Banks,” *IEEE Trans. Biomed. Eng.*, vol. 46, no. 2, pp. 192–202, 1999.

[15] Y. Min, H. Kim, S. Member, Y. Kang, G. Kim, J. Park, and S. Kim, “Design of Wavelet-Based ECG Detector for Implantable Cardiac Pacemakers,” *IEEE Trans. Biomed. Circuits Syst.*, vol. 7, no. 4, pp. 426–436, 2013.

Published Manuscript Link: http//10.1109/IECBES.2016.7843454

978-1-4673-7791-1/16/$31.00 ©2016 IEEE